

The effective force NL3 revisited

G. A. Lalazissis^{1,3}, S. Karatzikos^{1,3}, R. Fossion¹, D. Pena Arteaga³, A. V. Afanasjev², P. Ring^{1,3}

¹ *Department of Theoretical Physics, Aristotle University of Thessaloniki, GR-54124, Greece*

² *Department of Physics and Astronomy, Mississippi State University, Mississippi State, Mississippi 39762, USA and*

³ *Physik-Department, Technische Universität München D-85747, Garching, Germany*

Covariant density functional theory based on the relativistic mean field (RMF) Lagrangian with the parameter set NL3 has been used in the last ten years with great success. Now we propose a modification of this parameter set, which improves the description of the ground state properties of many nuclei and simultaneously provides an excellent description of excited states with collective character in spherical as well as in deformed nuclei.

PACS numbers: 21.10.-k, 21.60.-n, 24.10.Cn, 21.30.Fe, 21.60.Jz, 24.30.Gz

Density functional theory is a universal and powerful tool for describing properties of finite nuclei all over the periodic table. In the non-relativistic framework the most successful density functionals are the ones based on density dependent forces, such as the Skyrme [1] or the Gogny [2] functional. Relativistic mean field (RMF) theory was first introduced as a fully fledged quantum field theory by Walecka [3, 4]. However, it turned out very soon [5], that for a quantitative description of nuclear surface properties an additional density dependence is necessary. Nowadays RMF theory modified in this form is considered as a covariant form of density functional theory. Over the years it has gained considerable interest, in particular, for the description of nuclei at and far from stability [6, 7, 8, 9, 10]. Compared with non-relativistic density functionals covariant density functional theory has certain advantages. They are characterized by a new saturation mechanism obtained by a delicate balance between a strongly attractive scalar field and a strongly repulsive vector field. Moreover, the very large spin-orbit splitting, observed in finite nuclei, is a relativistic effect. Therefore, its treatment in relativistic models arises in a natural way without any additional adjustable parameters. In addition, time-odd mean fields which are important in systems with broken time reversal symmetry are uniquely defined in RMF theory because of the Lorentz covariance of the underlying Lagrangian [11].

Pairing properties are essential for a description of nuclei with open shells. They have been included first in the constant gap approximation by occupation numbers of BCS-type [12]. Since this procedure requires the knowledge of the experimental pairing gaps, it cannot be applied in unexplored regions of the nuclear chart, where the binding energies are not known. In addition, it is noted that the BCS approximation breaks down in nuclei far from the valley of stability, where the coupling to the continuum is essential [13]. Therefore the constant gap approximation has been replaced by relativistic Hartree-Bogoliubov (RHB) theory [14] which includes a finite range particle-particle interaction of Gogny form. The details of this theory have been discussed in several review articles [6, 7, 8] and in the references given there.

In any case the adopted functionals are considered uni-

versal in the sense that they can be used for nuclei all over the periodic table, where mean field theory is applicable. It is therefore very desirable to find a unique parameterization for the Lagrangian of the model, which is able to describe as many experimental data as possible. In other words, we search for an effective force that is able to describe properties of nuclei from light to very heavy, from the proton to the neutron drip line. Moreover, a powerful density functional should not only describe the ground state properties of finite nuclei but also, at the same time, collective excited states within time-dependent density functional theory. This is crucial because otherwise, one would end up with one effective force for the description of the masses, another one for exotic systems, a third one for giant resonances and so on. Definitely, such specific parameterizations do not serve the purposes of universal density functional theory. Their inability originates from the fact that they are tailored to describe either specific observables or narrow regions of the periodic chart.

There are several types of relativistic density functionals. Conventional RMF theory is based on the Walecka model, where the nucleons interact by the exchange of phenomenological mesons and, up to now, in all the successful relativistic models two additional assumptions are essential: (i) in the *mean field approximation* only the nucleonic fields are quantized and the nucleons move independently in classical mesons fields, depending in a self-consistent way on the nuclear densities and currents, and (ii) in the *no-sea approximation* vacuum polarization and the contributions of the negative energy solutions are not explicitly taken into account.

Of course, the pure Walecka model is unable to describe nuclear matter and finite nuclei in a quantitative way. The medium dependence induced by many-body correlations is not reproduced properly. This leads to an effective density dependence, which can be taken into account either by non-linear self-interactions between the mesons or by a density dependence of the coupling constants. Models with density dependent coupling constants are tailored more in the spirit of density functional theory. Indeed, they have turned out to be very successful [15, 16, 17]. However, they are technically more

TABLE I: The experimental values of the energies of the Giant Monopole (GMR) and Giant Dipole (GDR) Resonances in ^{208}Pb are compared with the predictions of various non-linear forces.

	Exp.	NL3	NL3*	NL-SH	NL-1	NL-Z	NL-RA1
GMR	14.1 ± 0.3	14.04	13.90	16.48	12.44	11.72	15.26
GDR	13.3 ± 0.1	12.95	12.95	12.98	12.97	12.53	12.87

complicated, in particular, for RPA calculations. On the other hand, non-linear models have some justification. In fact, the effects of vacuum polarization which can contribute up to 30 % to the resulting binding energies are not taken into account explicitly in the framework of the no-sea approximation, but only globally by adjusting the parameters of the model. A proper renormalization procedure in nuclear matter [18] and in finite nuclei [19, 20, 21] leads to counterterms in the form of non-linear meson coupling. From this point of view non-linear meson coupling theories seem at a first glance to be more appropriate for a phenomenological description of vacuum polarization as compared to those using density dependent coupling constants. Of course, by adjustment of the final Lagrangian to the same experimental data, both methods to introduce a density dependence lead to very similar results. However the details are different: non-linear meson couplings lead in the case of nuclear matter to density dependent meson masses, i.e. to density dependent range parameters of the force and no rearrangement terms in the Dirac equation, whereas density dependent coupling constants lead to density dependent strength parameters of the effective force and additional rearrangement terms. So far such differences have not been investigated in detail.

The parameter set NL3 [22] with non-linear meson couplings represents one of most successful non-linear RMF forces. It was proposed ten years ago. In the meantime, new experimental data on nuclear masses have appeared. Moreover, new and more reliable information about the neutron skin became available. On the other hand, it was found that NL3 encounters some difficulties in describing light Hg and Pb isotopes [23] and certainly, there is always a need for better predictions of the masses which, of course, reflect also correct nuclear sizes. For this reason we decided to improve the parameter set NL3 by performing a new global fit of ground state properties of spherical nuclei and infinite nuclear matter. New parameterization obtained in this fit will be called NL3*.

In order to stay as close as possible to the very successful parameter set NL3, we kept in this fit the functional form of the Lagrangian unchanged. In particular the density dependence of the both parameter sets NL3 and NL3* is determined by the non-linear meson couplings in the isoscalar channel σ . We will discuss the adequacy of this ansatz at the end of this letter.

The starting point of Covariant Density Functional

Theory (CDFT) is a standard Lagrangian density [24]

$$\begin{aligned} \mathcal{L} = & \bar{\psi}(\gamma(i\partial - g_\omega\omega - g_\rho\vec{\rho}\vec{\tau} - eA) - m - g_\sigma\sigma)\psi \\ & + \frac{1}{2}(\partial\sigma)^2 - \frac{1}{2}m_\sigma^2\sigma^2 - \frac{1}{4}\Omega_{\mu\nu}\Omega^{\mu\nu} + \frac{1}{2}m_\omega^2\omega^2 \\ & - \frac{1}{4}\vec{R}_{\mu\nu}\vec{R}^{\mu\nu} + \frac{1}{2}m_\rho^2\vec{\rho}^2 - \frac{1}{4}F_{\mu\nu}F^{\mu\nu} \end{aligned} \quad (1)$$

which contains nucleons described by the Dirac spinors ψ with the mass m and several relativistic fields characterized by the quantum numbers of spin, parity, and isospin. These are effective fields mediated by mesons, with no direct connection to mesons and resonances existing in free space. They only carry their quantum numbers and characterize the properties of the possible relativistic fields entering the effective Dirac equation, which corresponds to the Kohn-Sham equation [25] in the non-relativistic case. It is only for simplicity that we use the conventional names σ ($I^\pi = 0^+, T = 0$), ω ($I^\pi = 1^-, T = 0$), and ρ ($I^\pi = 1^-, T = 1$). In addition, we have the electromagnetic field A . In principle there should also be an effective scalar meson with $I^\pi = 0^+$, and $T = 0$, the δ -meson. It plays an important role in G-matrix calculations [26]. However, present phenomenological parameterizations of the relativistic energy density functional [16, 17, 22] are very successful without the inclusion of this meson. On the basis of present experimental data in finite nuclei it is very difficult to distinguish between effective scalar and vector mesons in the isospin $T = 1$ channel, and, therefore, all the isospin dependence is carried by the effective ρ -meson.

The Lagrangian (1) contains as parameters the meson masses m_σ , m_ω , and m_ρ and the coupling constants g_σ , g_ω , and g_ρ . This model has first been introduced by Walecka [3, 4]. It soon became clear that surface properties of finite nuclei, in particular, the incompressibility, cannot be described properly by this model. Therefore, Boguta and Bodmer [5] introduced a non-linear meson coupling

$$U(\sigma) = \frac{1}{2}m_\sigma^2\sigma^2 + \frac{1}{3}g_2\sigma^3 + \frac{1}{4}g_3\sigma^4. \quad (2)$$

which brings in an additional density dependence. By fitting experimental data of some carefully chosen spherical nuclei, very successful parameter sets have been proposed. For example, the set NL1 [12] is an excellent force for describing ground state and rotational properties of finite nuclei along the valley of stability. However, it produces a very large asymmetry parameter a_4 . Therefore,

TABLE II: The total binding energies B.E., charge radii r_c , and the differences between the radii of neutron and proton density distributions $r_{np} = (r_n - r_p)$, used to adjust the new parameter set NL3*. The calculated values are compared with experimental data (values in parentheses).

	B.E.(MeV)	r_c (fm)	r_n-r_p (fm)
^{16}O	-128.112(-127.619)	2.735(2.730)	-0.15
^{40}Ca	-341.578(-342.052)	3.470(3.485)	-0.14
^{48}Ca	-413.615(-415.990)	3.470(3.484)	0.14
^{72}Ni	-612.168(-613.152)	3.892	0.26
^{90}Zr	-782.368(-783.891)	4.263(4.272)	0.04 (0.07)
^{116}Sn	-986.512(-988.680)	4.604(4.626)	0.10 (0.12)
^{124}Sn	-1048.324(-1049.962)	4.655(4.674)	0.22 (0.19)
^{132}Sn	-1101.550(-1102.850)	4.636	0.29
^{204}Pb	-1608.100(-1607.505)	5.432(5.486)	0.19
^{208}Pb	-1638.230(-1636.430)	5.508(5.505)	0.23 (0.20)
^{214}Pb	-1660.119(-1663.290)	5.566(5.562)	0.26
^{210}Po	-1649.024(-1645.210)	5.544	0.20

later, the parameter set NL3 [22] was introduced to improve the asymmetry parameter using the same ansatz without increasing the number of phenomenological parameters. This set is able to describe many ground state properties of finite nuclei all over the periodic table. Recently, the set NL3 has also been applied very successfully for the investigation of excited states such as collective rotations [27, 28, 29] and giant resonances [30, 31, 32, 33]. In particular, the use of the effective force NL3 in the ph -channel together with the Brink-Booker part of the Gogny force D1S in the pp -channel [14], within the framework of RHB theory, led to a very successful tool for the description of many properties of ground states as well as of excited states with collective character. The NL3 force was for a long time the only parameterization of the Lagrangian of the RMF theory that was able to provide simultaneously a consistent description of both excitation energies of giant monopole and giant dipole resonances.

In Table I, the experimental values of the energies of the Giant Monopole (GMR) and Giant Dipole Resonances (GDR) in ^{208}Pb are compared with the predictions of various non-linear forces. It is clearly seen that all forces give reasonable values for the GDR energy, which are close to experiment. This is not the case, however, for the giant monopole resonance. There, all forces predict values which, either overestimate (NL-SH [34] and NL-RA1 [35]) or underestimate (NL1 [12], NLZ [36]) the experimental value. Only NL3 and NL3* give results which are in excellent agreement with experiment. This, of course, is connected with the value of the incompress-

TABLE III: Parameters of the effective interaction NL3* in the RMF theory together with the nuclear matter properties obtained with this effective force. The values of nuclear matter properties obtained with NL3 are shown in parentheses.

Parameters of NL3*	
$M = 939$ (MeV)	
$m_\sigma = 502.5742$ (MeV)	$g_\sigma = 10.0944$
$m_\omega = 782.600$ (MeV)	$g_\omega = 12.8065$
$m_\rho = 763.000$ (MeV)	$g_\rho = 4.5748$
$g_2 = -10.8093$ (fm^{-1})	
$g_3 = -30.1486$	
Nuclear matter properties	
$\rho_0 = 0.150$	(0.148) fm^{-3}
$(E/A)_\infty = 16.31$	(16.30) MeV
$K = 258.28$	(271.76) MeV
$J = 38.6$	(37.4) MeV
$m^*/m = 0.594$	(0.60)

ibility of nuclear matter predicted by each of these forces.

The starting point for the fit of the new parameter set were the NL3 values, this time, however, the mass m_ω of the ω -meson was kept fixed to $m_\omega = 782.6$ MeV. This value differs slightly from that obtained in the NL3 fit in Ref. [22] and is the same as the one proposed for the free nucleon-nucleon force by Machleidt in Ref. [37]. As shown in Table II we used twelve spherical nuclei for the present fit: ^{16}O , ^{40}Ca , ^{48}Ca , ^{72}Ni , ^{90}Zr , ^{116}Sn , ^{124}Sn , ^{204}Pb , ^{208}Pb , ^{214}Pb , and ^{210}Po . Compared with the input for the NL3 fit in Ref. [22] we added the nuclei ^{204}Pb and ^{210}Po and replaced ^{58}Ni by ^{72}Ni in order to include more data on neutron rich isotopes. The experimental binding energies were taken from Ref. [38], and the charge radii from a recent compilation in Ref. [39]. The most recent experimental information on the neutron skins of the nuclei ^{90}Zr [40], ^{116}Sn , ^{124}Sn and ^{208}Pb [41, 42] was also included. The values in parentheses correspond to the relative error bars used in the fitting procedure. The binding energies of finite nuclei and the charge radii are taken within an uncertainty of 0.1% and 0.2%, respectively. The error used for the neutron skin is 5%.

For the open shell nuclei pairing correlations are treated in the BCS approximation with empirical pairing gaps (five-point formula). Nuclear matter information was also considered in the fit. The "empirical" input is: $E/A = -16$ MeV (5%), $\rho_0 = 0.153$ fm^{-3} (10%), $K_0 = 250$ MeV (10%), and $J = 33$ MeV (10%). The values in parentheses correspond to the error bars used in the fitting procedure. The resulting values of the Lagrangian parameterization NL3* are given in Table III, together with the predictions of the force for the nuclear matter properties at the saturation point. The values in parentheses are the predictions obtained with the ef-

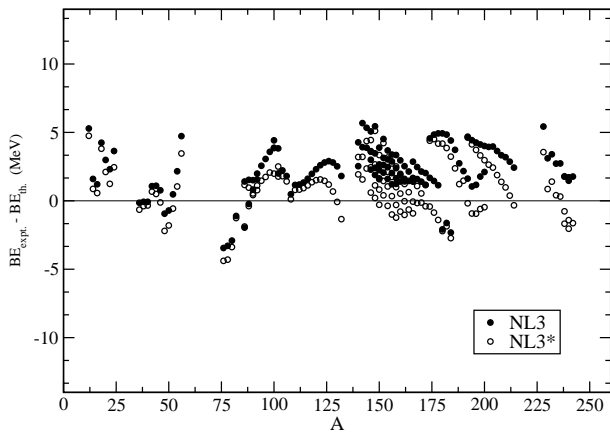


FIG. 1: Absolute deviations of the binding energies calculated with the parameter sets NL3 (filled circles) and NL3* (open circles) from the experimental values of Ref. [38].

fective interaction NL3. The resulting energy at saturation and asymmetry energy are rather close to the former values, only incompressibility is about 12 MeV smaller. Nonetheless both values are still somewhat too high as compared with other parameter sets with a density dependence in the iso-vector channel [43, 44].

In Fig. 1 the binding energies of more than 180 even-even nuclei are compared with experiment and the predictions of the NL3 forces. All calculations have been performed within the RHB model with the Gogny force D1S [45] in the pairing channel.

$$V^{pp}(1,2) = \sum_{i=1,2} e^{-\frac{r^2}{\mu_i^2}} (W_i + B_i P^\sigma - H_i P^\tau - M_i P^\sigma P^\tau). \quad (3)$$

The parameters μ_i , W_i , B_i , H_i , and M_i ($i = 1, 2$) of this force are given in Ref. [46]. It should be emphasized that, since a finite-range pairing interaction is used, the results do not depend on unphysical parameters like, the momentum cut-off in the pairing channel.

The results of NL3* are shown as open circles while those obtained with NL3 are marked by filled circles. For light nuclei, both forces give similar predictions, however, as the mass number increases NL3* results are clearly closer to the zero MeV line.

As discussed above the parameter set NL3 had difficulties to reproduce the proper ground state deformations in light Hg and Pb nuclei [23]. This is no longer the case with the parameter set NL3*. To investigate this, we have carried out constrained axially deformed RHB calculations of several even- A Pb isotopes with masses between $182 \leq A \leq 192$ in an external quadrupole field and we display in Fig. 2 the corresponding energy surfaces as a function of the quadrupole deformation. It is seen that in all cases the Pb isotopes turn out to be spherical. This is also the case for all other Pb isotopes, which are not shown in the figure. It is also seen that the Pb isotopes manifest the interesting effect of shape

coexistence. The energies which correspond to the oblate and prolate shape solutions are very close to the spherical ones but definitely lay higher in energy. This indicates a clear improvement as compared to the parameter set NL3, where some light Pb isotopes showed a deformed shape [23]. A more quantitative analysis goes beyond the mean field limit and requires, for instance, GCM-calculations [47, 48]. It is essential, however, that the mean field solution, which is the starting point for such investigations gives the correct behavior.

In the following we investigate dynamical processes such as collective vibrations with the same parameter set NL3*. For that purpose we study the time-dependent RMF or RHB equations in the small amplitude limit [49], i.e. we solve the relativistic RPA or QRPA equations. In Fig. 3 we display results for the monopole and isovector dipole response for the nucleus ^{208}Pb . For the multipole operator $\hat{Q}_{\lambda\mu}$ the response function $R(E)$ is defined

$$R(E) = \sum_i B(J_i \rightarrow 0_f) \frac{\Gamma/2\pi}{(E - E_i)^2 + \Gamma^2/4}, \quad (4)$$

where Γ is the width of the Lorentzian distribution, and

$$B(J_i \rightarrow 0_f) = \frac{1}{2J_i + 1} |\langle J_i || \hat{Q}_\lambda || 0_f \rangle|^2. \quad (5)$$

In the examples considered here the continuous strength distributions are obtained by folding the discrete spectrum of R(Q)RPA states with the Lorentzian (see Eq. (4)) with constant width $\Gamma = 0.5$ MeV [32]. The calculated peak energies of the ISGMR resonance at 13.9 MeV and of the IVGDR resonance at 12.95 MeV should be compared with the experimental excitation energies: $E = 14.1 \pm 0.3$ MeV [50] for the monopole resonance, and $E = 13.3 \pm 0.1$ MeV [51] for the dipole resonance, respectively. Clearly, the agreement with experiment is very good. The NL3 force predicts the same value for the IVGDR and a slightly larger value for the ISGMR. This is to be expected as the predicted value for the nuclear incompressibility with NL3 is larger than the one obtained with NL3*. However, both values are within the experimental error bars and one could say that RMF theory with non-linear meson couplings leads to values of the incompressibility around 260 ± 10 MeV.

Recently a new computer code has been developed for the solution of the relativistic QRPA equations in axially deformed nuclei [52, 53]. We used this code for the study of giant resonances in deformed nuclei. Here, we present as an example calculations in the prolate deformed nucleus ^{100}Mo . In Fig. 4 we show the total isovector dipole cross section as function of the GDR energy. The parameter set NL3* is very effective in reproducing these experimental data. The full line corresponds to the fully self-consistent deformed relativistic QRPA calculations while the dotted line are the experimental data [54, 55]. The estimated centroid energy for the GDR differs from the experimental value by less than 0.2 MeV. It is noted that NL3 also predicts excellent results, however, our analysis

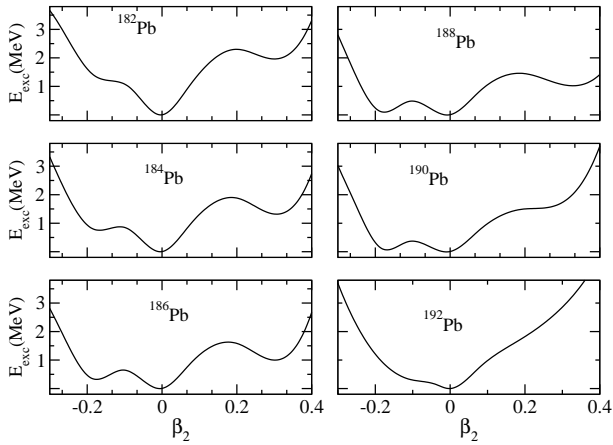


FIG. 2: Excitations energies of even-Pb isotopes as a function of the deformation parameter β_2 .

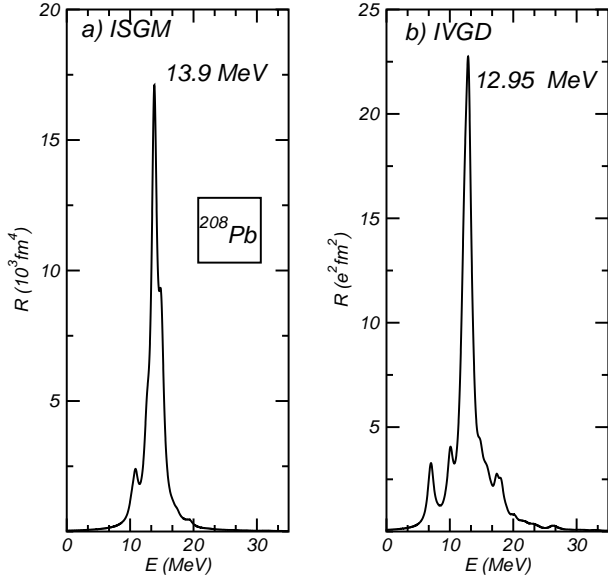


FIG. 3: The isoscalar monopole (a), and the isovector dipole (b) strength distributions in ^{208}Pb calculated with the effective interaction NL3*. The experimental excitation energies are 14.1 ± 0.3 MeV [50] for the monopole resonance, and 13.3 ± 0.1 MeV [51] for the dipole resonance, respectively.

shows that the results with the newly developed NL3* are slightly better. This can be traced back to the improvement in the density dependence of the non-linear sigma channel of the new force.

The response of the nuclei to an external force provides an important test of our understanding of their microscopic structure. The Coriolis force is one of such forces. It is of particular interest because it breaks time reversal symmetry in the intrinsic frame and leads therefore to currents and to nuclear magnetic fields having its origin in the spatial contributions of the vector mesons [56]. The impact of this field can be studied in rotat-

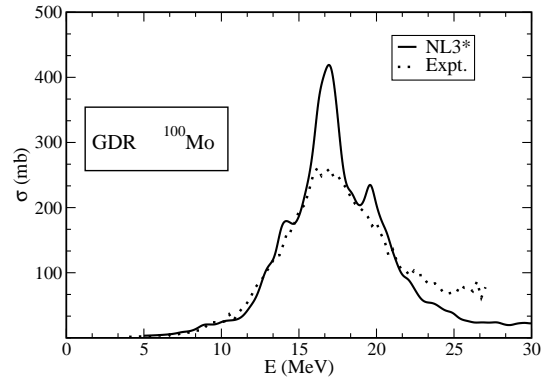


FIG. 4: The total isovector electric dipole cross section (in mb) of the deformed nucleus ^{100}Mo as a function of the excitation energy, calculated with the effective force NL3*, is compared with experiment [54, 55].

ing nuclei. Such studies were previously performed with various non-linear RMF parameterizations in the different parts of the nuclear chart, see Ref. [7] and references therein. In order to test the parameter set NL3* we selected several representative examples. This choice was guided by (i) the necessity to test the accuracy of the description of different types of rotational bands in different mass regions, and (ii) the restriction to consider only bands which are very weakly affected by the pairing correlations. The later constraint is related to the fact that the pairing modifies considerably the rotational properties and some inadequacies in the pairing channel may prevent meaningful conclusions about the reliability of the parameterization. For a discussion of this point see Ref. [28]. Thus, a highly-deformed band in the nucleus ^{58}Cu [57], a non-terminating ground state band in ^{74}Kr [58], a smoothly-terminating band in ^{109}Sb [59], and an yrast superdeformed (SD) band in ^{143}Eu [60] were selected for this comparison. The pairing correlations are weak in these bands, and thus all calculations were performed within the framework of cranked relativistic mean field (CRMf) theory [61] which neglects pairing.

The results of these calculations for rotational and deformation properties of the bands mentioned before are compared with experiment in Fig. 5. The kinematic ($J^{(1)}$) and dynamic ($J^{(2)}$) moments of inertia (Fig. 5a) of the highly-deformed band in ^{58}Cu as well as its transition quadrupole moment Q_t (Fig. 5e) are well described by the CRMf calculations. The fact that the $J^{(1)}$ moment is considerably larger than the $J^{(2)}$ moment and that both moments smoothly decrease with rotational frequency are clear fingerprints that the pairing is not important at high spin [7]. While this condition is clearly satisfied in ^{58}Cu (see Fig. 5a), these moments are closer to each other in the case of the SD band in ^{143}Eu (Fig. 5b) suggesting that the pairing is relatively more important in the later band. As a result, we observe somewhat larger discrepancies between experiment and theory in the case of ^{143}Eu (Fig. 5b). If the calculations would

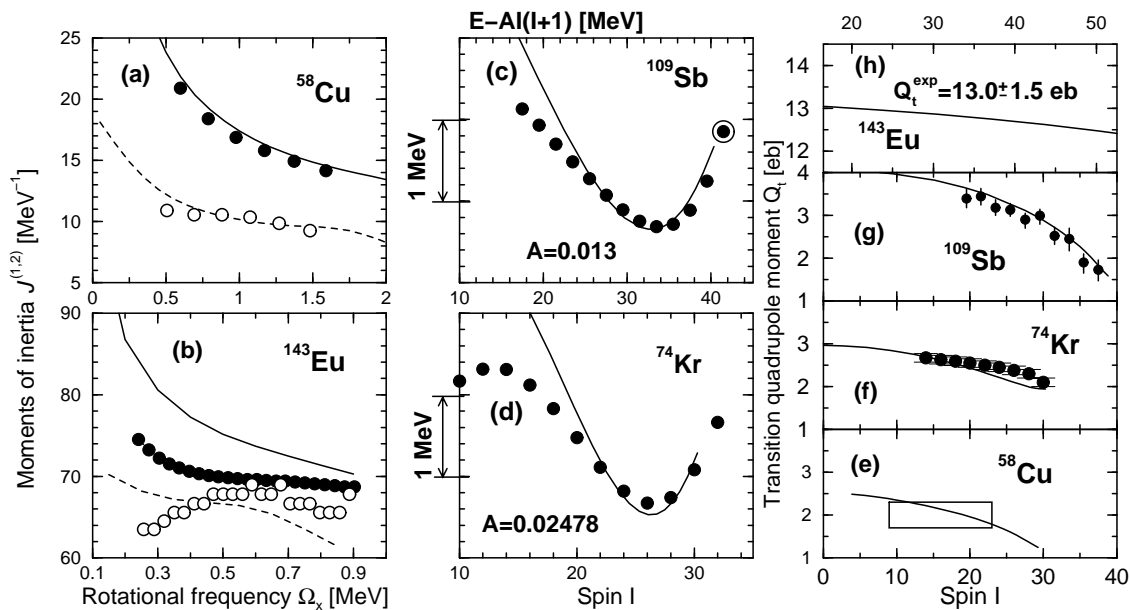


FIG. 5: Panels (a-b): Kinematic (solid circles, solid lines) and dynamic (open circles, dashed lines) moments of inertia in the highly-deformed band in ⁵⁸Cu and the yrast superdeformed band of ¹⁴³Eu. Experimental data are shown by circles, while the results of calculations by lines. Panels (c-d): Excitation energies of the non-terminating band in ⁷⁴Kr and the smoothly terminating band in ¹⁰⁹Sb relative to a rigid rotor reference $E_{RLD}(I) = AI(I+1)$, where A is a moment of inertia parameter. Panels (e-h): Experimental and calculated transition quadrupole moments Q_t . Only the data for ¹⁴³Eu include the errors due to the uncertainties in the nuclear and electronic stopping powers. Other data exclude these uncertainties which are on the level of 10-15% of absolute value of Q_t . The box in panel (e) indicates the upper and lower limits of Q_t and the spin range where they have been measured. The panel (h) itself acts as such a box in the case of the ¹⁴³Eu band. Experimental data are taken from Refs. [57] (⁵⁸Cu), [58] (⁷⁴Kr), [59, 62] (¹⁰⁹Sb), and [60] (¹⁴³Eu).

include weak pairing, this would lead to the decrease (increase) of calculated $J^{(1)}$ ($J^{(2)}$) moments of inertia bringing them closer to experimental data. It is also necessary to mention that the SD band in ¹⁴³Eu is not linked to the low-spin spectra.

Based on the effective alignment approach with respect of the linked yrast SD band in ¹⁵²Dy [7, 63] the spin of the initial state of this band has been suggested to be

$I_0 = 16.5\hbar$: this value has been used in the plotting of experimental kinematic moment of inertia in Fig. 5b. However, one cannot completely exclude also the value $I_0 = 18.5\hbar$ (see discussion in Ref. [61]); this would increase experimental $J^{(1)}$ values bringing them closer to calculated ones. The rotational properties of the bands which come close to their maximum spin I_{max} (as defined from the distribution of particles/holes over low- and high- j orbitals) are usually analyzed employing excitation energies plotted versus rigid rotor reference. This type of analysis is used for the bands in ¹⁰⁹Sb and ⁷⁴Kr, see Figs. 5c and 5d. One can see that at high spin above $I \sim 20\hbar$, where the pairing is expected to be weak, the CRMF results describe the excitation energies very well. The band in ¹⁰⁹Sb is a classical example of a smoothly terminating band; it starts at low spin at near-prolate shape, then with increasing spin its shape becomes more and more triaxial and finally at $I_{max} = 41.5\hbar$ it terminates in a non-collective oblate state [7]. This process

of smooth band termination is associated with the gradual loss of collectivity which is nicely seen in the drop of the transition quadrupole moment Q_t with increasing spin (see Fig. 5g). This feature is nicely reproduced in the calculations. On the contrary, the ground state band in ⁷⁴Kr reveals a new phenomenon of non-termination of rotational bands (see Ref. [58] for details): it remains collective at $I_{max} = 32\hbar$. Contrary to the case of the band in ¹⁰⁹Sb, its transition quadrupole moment is more constant as a function of spin (see Fig. 5f).

One can see that the CRMF calculations with the parameter set NL3* provide a very successful description of different aspects of rotating nuclei. In general, the results of the calculations are very close to the ones obtained earlier with the NL3 parameterization of the RMF Lagrangian.

As mentioned above, the density dependence of the parameter sets NL3 and NL3* is determined by the non-linear meson couplings in the isoscalar channel σ . The vector fields ω and ρ , in particular, the isovector channel described by the ρ -meson are still coupled linearly and this leads to relatively large neutron radii and a very stiff equation of state for neutron matter [16] as well as very stiff symmetry energies as a function of the density [44]. Models with non-linear couplings in the ρ -channel as for instance the parameter set FSUGold introduced by Piekarewicz in Ref. [64] can improve this, however at

the cost of additional parameters. Density dependent covariant functionals eliminate the non-linear coupling terms and use, instead of that, at the cost of additional parameters, density dependent coupling constants $g_\sigma(\rho)$, $g_\omega(\rho)$, and $g_\rho(\rho)$ which depend on the baryon density ρ . This concept is evidently closer to the idea of density functional theory. On the other hand, one has to keep in mind that a proper treatment of the effects of vacuum polarization by a renormalization procedure would require counterterms which are nonlinear in the meson fields with the same polynomial structure [18, 19, 20, 21]. In addition, because of the relatively small surface diffuseness in nuclear systems and the narrow range, in which the density is changing from its value at saturation to zero, calculations of matrix elements with density dependent coupling constants and of the corresponding rearrangement terms require a considerably larger numerical effort, in particular, in the case of axially symmetric and triaxial applications. Considering all these points the non-linear version of RMF theory is still a very useful concept because it combines simplicity with excellent predictions for many nuclear properties.

In conclusion, in the present work we have reconsidered the well known parameter set NL3 after ten years and by

a new fit with modern experimental data we introduced an improved parameterization NL3* for the RMF model, which contains only six phenomenological parameters. It is able to improve the description of nuclear masses and to cure some small problems observed previously with the NL3 force. At the same time, it provides excellent results for collective properties of vibrational and rotational character.

Acknowledgements

This work has been supported in part by the Gesellschaft für Schwerionenforschung (GSI), by the BMBF (Germany) under the project 06 MT246, by the DFG cluster of excellence “Origin and Structure of the Universe” (www.universe-cluster.de), by the Greek Ministry of National Education and Religious Affairs, in the framework of the Pythagoras II, EPEAEK II and E.U. project 80861, by the Hellenic State Scholarship foundation (IKY) and by the Department of Energy under award number DE-FG02-07ER41459.

-
- [1] D. Vautherin and D. M. Brink, *Phys. Rev.* **C5**, 626 (1972).
 - [2] J. Dechargé and D. Gogny, *Phys. Rev.* **C21**, 1568 (1980).
 - [3] J. D. Walecka, *Ann. Phys. (N.Y.)* **83**, 491 (1974).
 - [4] B. D. Serot and J. D. Walecka, *Adv. Nucl. Phys.* **16**, 1 (1986).
 - [5] J. Boguta and A. R. Bodmer, *Nucl. Phys.* **A292**, 413 (1977).
 - [6] P. Ring, *Prog. Part. Nucl. Phys.* **37**, 193 (1996).
 - [7] D. Vretenar, A. V. Afanasjev, G. A. Lalazissis, and P. Ring, *Phys. Rep.* **409**, 101 (2005).
 - [8] J. Meng, H. Toki, S.-G. Zhou, S.-Q. Zhang, W.-H. Long, and L.-S. Geng, *Prog. Part. Nucl. Phys.* **57**, 470 (2006).
 - [9] J. Piekarewicz, *Phys. Rev.* **C76**, 064310 (2007).
 - [10] R. J. Furnstahl, *Lecture Notes in Physics* (Springer-Verlag, Heidelberg, 2007), Vol. eprint arXiv:nucl-th/0702040.
 - [11] A. V. Afanasjev and P. Ring, *Phys. Rev.* **C62**, 031302(R) (2000).
 - [12] P.-G. Reinhard, M. Rufa, J. Maruhn, W. Greiner, and J. Friedrich, *Z. Phys.* **A323**, 13 (1986).
 - [13] J. Dobaczewski, H. Flocard, and J. Treiner, *Nucl. Phys.* **A422**, 103 (1984).
 - [14] T. Gonzales-Llarena, J. L. Egido, G. A. Lalazissis, and P. Ring, *Phys. Lett.* **B379**, 13 (1996).
 - [15] S. Typel and H. H. Wolter, *Nucl. Phys.* **A656**, 331 (1999).
 - [16] T. Nikšić, D. Vretenar, P. Finelli, and P. Ring, *Phys. Rev.* **C66**, 024306 (2002).
 - [17] G. A. Lalazissis, T. Nikšić, D. Vretenar, and P. Ring, *Phys. Rev.* **C71**, 024312 (2005).
 - [18] S. A. Chin, *Ann. Phys. (N.Y.)* **108**, 301 (1977).
 - [19] C. J. Horowitz and B. D. Serot, *Phys. Lett.* **B140**, 181 (1984).
 - [20] R. J. Perry, *Nucl. Phys.* **467**, 717 (1987).
 - [21] Z. Y. Zhu, H. J. Mang, and P. Ring, *Phys. Lett.* **B254**, 325 (1991).
 - [22] G. A. Lalazissis, J. König, and P. Ring, *Phys. Rev.* **C55**, 540 (1997).
 - [23] T. Nikšić, D. Vretenar, P. Ring, and G. A. Lalazissis, *Phys. Rev.* **C65**, 054320 (2002).
 - [24] Y. K. Gambhir, P. Ring, and A. Thimet, *Ann. Phys. (N.Y.)* **198**, 132 (1990).
 - [25] W. Kohn and L. J. Sham, *Phys. Rev.* **137**, A1697 (1965).
 - [26] M. Serra, T. Otsuka, Y. Akaishi, P. Ring, and S. Hirose, *Prog. Theor. Phys.* **113**, 1009 (2005).
 - [27] A. V. Afanasjev, J. König, P. Ring, J. L. Egido, and L. M. Robledo, *Phys. Rev.* **C62**, 054306 (2000).
 - [28] A. V. Afanasjev, T. L. Khoo, S. Frauendorf, G. A. Lalazissis, and I. Ahmad, *Phys. Rev.* **C67**, 024309 (2003).
 - [29] A. V. Afanasjev and S. Frauendorf, *Phys. Rev.* **C71**, 064318 (2005).
 - [30] D. Vretenar, H. Berghammer, and P. Ring, *Nucl. Phys.* **A581**, 679 (1995).
 - [31] D. Vretenar, G. A. Lalazissis, R. Behnsch, W. Pöschl, and P. Ring, *Nucl. Phys.* **A621**, 853 (1997).
 - [32] D. Vretenar, N. Paar, P. Ring, and G. A. Lalazissis, *Phys. Rev.* **C63**, 047301 (2001).
 - [33] D. Vretenar, N. Paar, P. Ring, and G. A. Lalazissis, *Nucl. Phys.* **A692**, 496 (2001).
 - [34] M. M. Sharma, M. A. Nagarajan, and P. Ring, *Phys. Lett.* **B312**, 377 (1993).
 - [35] M. Rashdan, *Phys. Rev.* **C63**, 044303 (2001).
 - [36] M. Rufa, P.-G. Reinhard, J. Maruhn, W. Greiner, and M. R. Strayer, *Phys. Rev.* **C38**, 390 (1988).

- [37] R. Machleidt, *Adv. Nucl. Phys.* **19**, 189 (1989).
- [38] G. Audi, A. H. Wapstra, and C. Thibault, *Nucl. Phys.* **A729**, 337 (2003).
- [39] E. G. Nadjakov, K. P. Marinova, and Y. P. Gangrsky, *At. Data Nucl. Data Tables* **56**, 133 (1994).
- [40] K. Yako, H. Sagawa, and H. Sakui, *Phys. Rev.* **C74**, 051303 (2006).
- [41] V. E. Starodubsky and N. M. Hintz, *Phys. Rev.* **C49**, 2118 (1994).
- [42] A. Krasznahorkay, M. Fujiwara, P. van Aarle, H. Akimune, I. Daito, H. Fujimura, Y. Fujita, M. N. Harakeh, T. Inomata, J. Jänecke, S. Nakajama, A. Tamii, M. Tanaka, H. Toyokawa, W. Uijen, and M. Yosoi, *Phys. Rev. Lett.* **82**, 3216 (1999).
- [43] J. Piekarewicz, *Phys. Rev.* **C66**, 034305 (2002).
- [44] D. Vretenar, T. Nikšić, and P. Ring, *Phys. Rev.* **C68**, 024310 (2003).
- [45] J. F. Berger, M. Girod, and D. Gogny, *Nucl. Phys.* **A428**, 23c (1984).
- [46] J. F. Berger, M. Girod, and D. Gogny, *Comp. Phys. Comm.* **61**, 365 (1991).
- [47] T. Nikšić, D. Vretenar, and P. Ring, *Phys. Rev.* **C73**, 034308 (2006).
- [48] T. Nikšić, D. Vretenar, and P. Ring, *Phys. Rev.* **C74**, 064309 (2006).
- [49] P. Ring, Z.-Y. Ma, N. Van Giai, D. Vretenar, A. Wandelt, and L.-G. Cao, *Nucl. Phys.* **A694**, 249 (2001).
- [50] D. H. Youngblood, H. L. Clark, and Y. W. Lui, *Phys. Rev. Lett.* **82**, 691 (1999).
- [51] J. Ritman, F.-D. Berg, V. Kühn, V. Metag, R. Novotny, M. Notheisen, P. Paul, M. Pfeiffer, O. Schwalb, H. Löhner, L. Venema, A. Gobbi, N. Herrmann, K. D. Hildenbrand, J. Mösner, R. S. Simon, K. Teh, J. P. Wessels, and T. Wienold, *Phys. Rev. Lett.* **70**, 533 (1993).
- [52] D. Pena Arteaga, Phd thesis, Technische Universität München (unpublished), 2007.
- [53] D. Pena Arteaga and P. Ring, *Phys. Rev.* **C77**, 034317 (2008).
- [54] H. Beil, R. Bergere, P. Carlos, A. Lepretre, A. de Miniac, and A. Veysiére, *Nucl. Phys.* **A227**, 427 (1974).
- [55] G. Rusev, E. Grosse, M. Erhard, K. Junghans, K. Kosev, K.-D. Schilling, R. Schwengner, and A. Wagner, *Eur. Phys. J.* **A27**, 171 (2006).
- [56] W. Koepf and P. Ring, *Nucl. Phys.* **A493**, 61 (1989).
- [57] D. Rudolph, C. Baktash, J. Dobaczewski, W. Nazarewicz, W. S. a, M. J. Brinkman, M. Devlin, H.-Q. Jin, D. R. LaFosse, L. L. Riedinger, D. G. Sarantites, and C.-H. Yu, *Phys. Rev. Lett.* **80**, 3018 (1998).
- [58] J. J. Valiente-Dobón, T. Steinhardt, C. E. Svensson, I. Ragnarsson, A. V. Afanasjev, C. Andreoiu, R. A. E. Austin, M. P. Carpenter, D. Dashdorj, G. de Angelis, J. E. F. Dönau, E. Farnea, P. Finlay, S. J. Freeman, A. Gadea, P. E. Garrett, A. Görge, G. F. Grinyer, B. Hyland, D. Jenkins, P. J. F. Johnston-Theasby, A. Jungclaus, K. P. Lieb, A. O. Macchiavelli, F. Moore, G. Mukherjee, D. R. Napoli, A. A. Phillips, C. Plettner, W. Reviol, D. Sarantites, H. Schnare, M. A. Schumaker, R. Schwengner, D. Seweryniak, M. B. Smith, I. Stefanescu, R. W. O.Thelen, and D. Ward, *Phys. Rev. Lett.* **95**, 232501 (2005).
- [59] H. Schnare, D. R. LaFosse, D. B. Fossan, J. R. Hughes, P. Vaska, K. Hauschild, I. M. Hibbert, R. Wadsworth, V. P. Janzen, D. C. Radford, S. M. Mullins, C. W. Beausang, E. S. Paul, J. DeGraaf, A. V. Afanasjev, and I. Ragnarsson, *Phys. Rev.* **C54**, 1598 (1996).
- [60] S. A. Forbes, A. Atac, G. B. Hagemann, B. Herskind, S. M. Mullins, P. J. Nolan, J. Nyberg, M. J. Piiparinen, G. Sletten, and R. Wadsworth, *Nucl. Phys.* **A584**, 149 (1995).
- [61] A. V. Afanasjev, J. König, and P. Ring, *Nucl. Phys.* **A608**, 107 (1996).
- [62] R. Wadsworth, R. M. Clark, J. A. Cameron, D. B. Fossan, I. M. Hibbert, V. P. Janzen, R. Krücken, G. J. Lane, I. Y. Lee, A. O. Macchiavelli, C. M. Parry, J. M. Sears, J. F. Smith, A. V. Afanasjev, and I. Ragnarsson, *Phys. Rev. Lett.* **80**, 1174 (1998).
- [63] A. V. Afanasjev, G. A. Lalazissis, and P. Ring, *Nucl. Phys.* **A634**, 395 (1998).
- [64] B. G. Todd-Rutel and J. Piekarewicz, *Phys. Rev. Lett.* **86**, 122501 (2005).